1-1-2013

Surface modification of polypyrrole/biopolymer composites for controlled protein and cellular adhesion

Paul J. Molino
University of Wollongong, pmolino@uow.edu.au

Binbin Zhang
University of Wollongong, bz107@uowmail.edu.au

Gordon G. Wallace
University of Wollongong, gwallace@uow.edu.au

Timothy Hanks
University of Wollongong, tim.hanks@furman.edu

Surface modification of polypyrrole/biopolymer composites for controlled protein and cellular adhesion

Abstract

The ability to control the interaction between proteins and cells with biomaterials is critical for the effective application of materials for a variety of biomedical applications. Herein, the surface modification of the biological dopant dextran sulphate-doped polypyrrole (PPy-DS) with poly(ethylene glycol) to generate a biomaterial interface that is highly resistant to protein and cellular adhesion is described. Thiolated poly(ethylene glycol) (PEG-thiol) was covalently bound to PPy-DS backbone via a thiol-ene reaction. The surface resistance to an extracellular matrix protein fibronectin increased with increasing molecular weight and concentration of PEG-thiol, and was further optimised via increasing the reaction temperature and the pH of the reactant aqueous solution. Optimised surface modification conditions substantially reduced interfacial protein adsorption, with the complete inhibition of adhesion and colonisation by primary mouse myoblasts. PEG-thiol-modified inherently conducting polymers are highly protein resistant multifunctional materials that are promising compounds for a range of biomedical and aquatic applications

Keywords

modification, surface, adhesion, cellular, protein, controlled, composites, biopolymer, polypyrrole

Disciplines

Engineering | Physical Sciences and Mathematics

Publication Details

Molino, P. J., Zhang, B., Wallace, G. G. and Hanks, T. (2013). Surface modification of polypyrrole/biopolymer composites for controlled protein and cellular adhesion. Biofouling, 29 (10), 1155-1167.

Surface Modification of Polypyrrole/Biopolymer Composites for Controlled Protein and Cellular Adhesion

Paul J. Molino[1]*, BinBin Zhang[1], Gordon G. Wallace[1] and Timothy W. Hanks[1,2]

[1]ARC Centre of Excellence for Electromaterials Science, Intelligent Polymer Research Institute, AIIM Facility, Innovation Campus, University of Wollongong, Wollongong, NSW 2522, Australia.

[2] Department of Chemistry, 3300 Poinsett Hwy, Furman University, Greenville, SC 29613.

*Author for correspondence: Dr Paul J Molino, pmolino@uow.edu.au; tel= (+61) 242981449; fax= (+61) 4221 3114

Word Count

Text: 6638

References: 1115

Figures: 341

TOTAL: 8094

Abstract

The ability to control the interaction between proteins and cells with biomaterials is critical for the effective application of materials for a variety of biomedical applications. Herein we describe the surface modification of biological dopant dextran sulphate doped polypyrrole (PPy-DS) with poly(ethylene glycol) (PEG) to generate a biomaterial interface that is highly resistant to protein and cellular adhesion. Thiolated poly(ethylene glycol) (PEG-thiol) was covalently bound to PPy-DS backbone via a *thiol-ene* reaction. The surface resistance to an extracellular matrix protein fibronectin (FN) increased with increasing PEG-thiol molecular weight and concentration, and was further optimised via increasing the reaction temperature and the pH of the aqueous reaction solution. Optimised surface modification conditions dramatically reduced interfacial protein adsorption, with the adhesion and colonisation by primary mouse myoblasts completely inhibited. PEG-thiol modified inherently conducting polymers (ICPs) are highly protein resistant multifunctional materials that are promising for a range of biomedical and aquatic applications.

Keywords. Electroactive Polymer, Polypyrrole, Protein adsorption, Fibronectin, Cell adhesion, Poly(ethylene glycol).

1. Introduction

The surface properties of materials that are in contact with biological media largely determine the biological response to the object. Considerable effort has been, and continues to be, made to minimize (or in some cases, maximize) protein deposition onto synthetic surfaces ranging from ocean vessel hulls to biological implants and tissue constructs (Ma et al. 2007). For example, biofouling in marine environments dramatically increases the fuel consumption of the world's navel fleets and contributes to increased structural loads and fatigue of marine structures such as oil platforms (Bixler & Bhushan 2012). Biofouling reduces flow in piping and membranes, encourages the contamination of water systems and food processing equipment, and generally decreases the efficiency of environmentally-exposed machinery and equipment. In the field of medical implants, bioadhesion reduces the lifetime of prostheses, leads to infections associated with catheters and ventilators, and can degrade the performance of sensing platforms (Palacio & Bhushan 2012). Bacterial biofilms are particularly problematic as they are highly resistant to the host's immune systems and antibiotics (Glinel et al. 2012).

Tissue engineering constructs and certain implants are particularly challenging materials to surface modify, as blanket resistance to adhesion of biological species is self-defeating. Instead, the goal is to encourage the growth of cells on and into the structure in a controlled manner (Meyers & Grinstaff 2012). In addition to controlling the bulk physical and chemical properties, the surfaces also need to be fashioned so that cells not only adhere to the surface, but do so in way that encourages directional growth in order to rebuild functional tissue. The two major strategies for doing this are to create custom surface topologies and chemical gradients (Alves et al. 2010, Falconnet et al. 2006, Lühmann & Hall 2009, Vladkova 2010). For example, consider structures designed to support neuronal cells. Here, the cells are

polarized, with dendrites on one end and axons on the other. These cells rely on topological, chemical and electrical cues to determine their orientation and direction of growth, which can only be fabricated by sophisticated material engineering strategies (Geckil et al. 2010, Khan & Newaz 2010, Roach et al. 2010, Yu et al. 2008).

Polysaccharides, particularly in the form of hydrogels, are attractive substrates for tissue engineering scaffolds due to their variety, biocompatibility, bioerodability, adjustable viscoelasticity, and relative ease of fabrication into macroscopic shapes (Aizawa et al. 2012, Zhang & Kohn 2012). These materials can be chemically modified to change their bulk and surface properties, and they have been shown to effectively encapsulate drugs and growth factors (Patil et al. 2010). Recently, carbohydrate polymers have been combined with intrinsically conducting polymers (ICPs) to create composites that are uniquely suited for interacting with biological systems. ICPs such as polypyrrole (PPy) and poly(ethylenedioxythiophene) show good biocompatibility and have found use in biomedical applications such as controlled release of bioactive compounds, actuators, and electrode coatings (Abidian & Martin 2009, Green et al. 2008, Ravichandran et al. 2010, Svirskis et al. 2010).

We are interested in the surface properties of ICP-biopolymer composites, particularly their interactions with proteins and cells (Gelmi et al. 2010, Higgins et al. 2012, Molino et al. 2012a). There are several ways in which the surfaces can be modified to alter the propensity for biomolecules to adsorb onto these surfaces, including chemical modification of the ICP or its dopant, chemical modification of the polysaccharide biopolymer, the entrapment of additives or growth conditions that alter the surface roughness. None of these methods are particularly useful for the preparation of materials with gradated or patterned surface

properties. Of particular interest would be an approach that would allow for precise spatial control using technologies such as inkjet or contact printing (Alves et al. 2010, Falconnet et al. 2006, Lühmann & Hall 2009, Vladkova 2010).

We have shown that the surface properties of ICPs, either with conventional dopants or in composites with carbohydrate biopolymers, can be modified by exposure to thiols (Bergman & Hanks 2000, Hanks et al. 2005, Molino et al. 2012b). The thiols may be in solution or in the gas phase and the extent of reaction depends upon exposure time. Thiols with hydrocarbon or fluorocarbon tails greatly increase the surface hydrophobicity and the fluorocarbon thiols impart modest resistance to the non-specific adsorption of fibronectin. Here, we examine the effectiveness of various reaction parameters on the deposition of thiol-terminated polyethylene glycols onto polypyrrole-dextran sulphate ionomer composites and the resistance of the resulting surfaces to the adsorption of the protein fibronectin and the adhesion of mammalian cells. Identification and optimization of key reaction parameters will assist in the fabrication of chemically patterned films and 3D constructs.

2. Experimental

2.1. General

Pyrrole was purchased from Merck, purified by distillation over molecular sieves and under nitrogen. It was then stored at -18 ºC. All other reagents were used as received. Dextran sulphate sodium salt (D-6001) and phosphate-buffered saline were purchased from Sigma-Aldrich (Sydney, Australia). Methoxy Poly(ethyleneglycol) thiol of 5k, 20k and 40k Molecular Weights (MWs) were purchased from JenKem Technology (USA), while a 1k MW PEG thiol was purchased from Sigma-Aldrich (729108). Human plasma fibronectin was

purchased from Invitrogen (Australia) (33016-015) and reconstituted in distilled water at a concentration of 1mg/ml and stored at -80 ºC prior to use.

2.2 Electrochemical Polymerisation of Polymer Films

Electrochemical polymerisation of conducting polymer films was performed using a Q-Sense Electrochemistry Module (QEM 401) axial flow cell with a Q-Sense E4 Quartz Crystal Microbalance system (Q-Sense AB, Västra, Frölunda, Sweden). The QCM sensor was an A-T cut quartz crystal with a 10 mm diameter gold electrode (QSX301) with a fundamental resonance frequency of 5 MHz (Q-Sense AB, Västra, Frölunda, Sweden). Prior to each experiment, the gold sensor surface upon the quartz crystal was cleaned with piranha solution (concentrated sulphuric acid: 30% hydrogen peroxide (7:3)) for 3 min, and then rinsed thoroughly with deionised water and dried with nitrogen gas. Aqueous solutions for polymer synthesis consisted of 0.2M pyrrole in deionised water with a 2mg/ml concentration of the counterion DS. Each solution was deoxygenated for 10 mins via bubbling with nitrogen gas before use. The Q-Sense electrochemistry cell consisted of a platinum counter electrode, and a World Precision Instruments® Dri-RefTM reference electrode, and gold working electrode upon the quartz sensor. PPy-DS films were grown galvanostatically onto gold coated Q-Sense quartz sensors using an eDAQ e-corder 410 recorder and EA163 potentiostat connected to the Q-Sense electrochemistry module. Aqueous polymer growing solution was flowed through the electrochemistry module at 60µl/min, and films grown at a current density of 0.25mA/cm^2 for 2 mins (charge density of 0.03 C/cm^2). Thereafter, the quartz sensors were removed from the E-cell and rinsed in deionised water and dried under a flow of nitrogen gas.

2.3 Film Characterization

2.3.1 Atomic Force Microscopy Topography

The surface morphology of the polymer films were examined using a Mikromash NSC15 cantilever (spring constant ~ 37 N/m) in AC mode with an MFP-3D AFM (Asylum Research, CA). Image scans of 5 µm were obtained at a scan rate of 0.5 Hz in air. Roughness and surface area values were calculated using Asylum Research Analysis software with the Igor Pro Software Package (WaveMetrics, OR).

2.4 Poly(ethylene glycol) - Thiol Modification of PPy-DS films

2.4.1 Thiol Molecular Weight, Concentration and Reaction Temperature

Thiol solutions of differing MWs (1k, 5k, 20k and 40k) were employed to test the influence of thiol MW, concentration and temperature on the degree of reaction to the PPy-DS polymer films using QCM-D. Electrochemically polymerized PPy-DS films were placed in standard Q-Sense flow modules (QFM 401) and equilibrated in deionised water for 60 mins.

To test the effect of thiol concentration on PEG-thiol modification and protein resistance, PEG-thiol concentrations of 0.1mM, 1mM and 10mM were prepared in deionised water and introduced to the flow modules at 30µl/min for 60 mins, and thereafter rinsed with deionised water at 30µl/min until the *f* and *D* measurement parameters stabilized. During PEG-thiol modification the temperature in the QCM flow modules was kept constant at 25 ± 0.02ºC. Thereafter the temperature was set at 22 ± 0.02°C and PBS introduced into the flow module for at least 60 mins until the *f* and *D* measurement parameters stabilized. A 50µg/ml solution of fibronectin (FN) in PBS (pH 7.4) was then introduced to the axial flow sample chamber and kept at a constant flow rate of 10µl/min for 60 mins, and then rinsed with fresh PBS at a rate of 30 µl/min until the QCM measurement parameters stabilised.

The Q-tools software package v.3.0.10.286 (Biolin Sci, AB) was used to apply the Voigt model to determine the mass (ng/cm^2) of PEG –thiol and protein adsorbed to the modified sensor surface. Specific model input parameters for PEG-thiol binding and protein adsorption quantification include layer density ((1027kg/m^3 - PEG-thiol), (1150kg/m^3 - FN)), fluid density (1020kg/m^3), layer viscosity ($1^{-6} \leq 1^{-2}$ kg/ms), layer shear modulus ($1^4 \leq 1^7$ Pa), and mass ($115 \leq 1.15^5$ ng/cm^2). The 5th, 7th and 9th overtones were used for all modelling calculations. QCM-D measurements include mass contributions from both the adsorbant (protein or PEG-thiol), and the water hydrodynamically coupled, or trapped, with the adsorbed molecules, and therefore hereafter references to the adsorbed mass (Δm) refer to the 'hydrated' molecular mass adsorbed to the polymer surface.

To test the influence of temperature on PEG-thiol modification, PPy-DS films were placed in standard Q-Sense flow modules (QFM 401) and equilibrated in distilled water for 60 mins at a constant temperature of either 15, 25, 35 or 45 ± 0.02 °C. At each temperature, solutions of 0.1mM PEG-thiol in deionised water were introduced into the flow cell at a rate of 30 µl/min for 60 mins, and thereafter rinsed at 30 µl/min with distilled water until the *f* and *D* parameters stabilized. Protein adsorption experiments were then undertaken as described above. Reaction temperature experiments were undertaken for each of 1k, 5k, 20k and 40k MW PEG-thiols.

2.4.2 Effect of Solvent

PEG-thiol (20k MW) solutions at 0.1mM concentration were made in either deionised water or ethanol. QCM-D sensor crystals (both piranha cleaned gold and PPy-DS modified as described in *section 2.2*) were mounted in standard QFM 401 flow cells and allowed to equilibrate in their respective solvent for 60 mins.

Thereafter 0.1mM PEG-thiol solution was introduced into the flow cell at 30ul/min for 60 mins, then rinsed with the solvent without PEG-thiol until the *f* and *D* parameters stabilised. Thereafter PBS was flowed into the flow cells and the system left to equilibrate. Protein adsorption studies using FN were then performed as described in *section 2.4.1*.

2.4.3 Phosphene Catalysts

PEG-thiol (20k MW) solutions at 0.1mM concentration were prepared in deionized water with either 0.005 or 0.02 mM Tris(2-Carboxyethyl)phosphine, hydrochloride (TCEP). The degree of the thiol-polymer reaction was followed using QCM-D at 25 °C, and FN adsorption experiments were undertaken thereafter, following standard experimental protocols described above. Films treated with TCEP without thiol acted as the experimental control.

2.4.4 Addition of Base

100mM aqueous solutions of di-sodium hydrogen orthophosphate solutions were prepared and buffered to pH values of 8, 9 and 10 using concentrated hydrochloric acid or sodium hydroxide as required. The buffers were used to prepare 0.1mM solutions of PEG (20k MW), with PEG-thiol modification and FN-adsorption studies undertaken following the standard protocols set out in *section 2.4.2*. The temperature during PEG-thiol modification was kept constant at 25 ± 0.02 ºC.

2.5 Cellular Adhesion Assay

PPy-DS films were electrochemically polymerised at 0.25mA/cm^2 for 2 mins on 18 x18 mm glass coverslips coated with 3nm Ti and 30nm Au using a sputter coater. The PPy-DS coated electrodes were then semi-immersed in an aqueous solution containing 1mM 40k MW PEG-

thiol, buffered to pH 9 using di-sodium hydrogen orthophosphate, and heated to a temperature of 45°C. After 60 mins incubation, the films were rinsed thoroughly with deionised water and dried with flowing nitrogen gas. Films were then sterilised with 70% ethanol solution, left to dry in a sterile 6 well plate in a biosafety cabinet, and incubated with sterile HAMS F10 cell culture media containing 20% fetal bovine serum. After 12 hrs incubation, 30,000 cells/cm^2 were seeded onto the samples and placed in a cell growth chamber at 37°C and 5% CO_2. After 3 days, samples were rinsed with sterile PBS and fixed in 3.7% paraformaldehyde solution, and imaged using a Zeiss Axiovert inverted microscope.

3. Results

3.1 Surface Topology

Growth of the PPy-DS films on the gold substrate was initiated galvanostatically. The potential drawn was constant during polymer growth at +650 mV indicating deposition of a conducting material. The PPy-DS films were subsequently modified according to the reaction described in Figure 1.

Measuring the interfacial surface area enables the normalisation of the PEG-thiol and FN binding density to the actual polymer surface area. AFM topographic representations of the PPy-DS polymer surface reveal a nodular polymer morphology typical of polypyrrole films (Figure 2). Polymer surface roughness, as measured directly from the AFM topographic scan, is 9.8 ± 0.57 nm (R_{RMS} roughness), with the interfacial surface area increasing, compared to a geometrically flat AFM scan area, by 4.1 ± 0.07 %. The PEG-thiol modification does not alter the surface roughness of the polymer as measured using optical profilometry (data not shown).

3.2 PEG Modification of PPy Films

3.2.1 PEG-thiol Molecular Weight and Concentration

Figure 3 illustrates PEG-thiol mass binding as a function of PEG MW and concentration (a), and the subsequent mass of FN adsorption to the respective modified PPy-DS films (b). PEG-thiol binding mass increased as a function of increasing MW (1k < 5k < 20k < 40k) and increasing concentration for all MWs. The impact of increasing PEG-thiol concentration was greatest for the 40k MW treatment, demonstrating binding of 1926, 2720 and 6197 ng/cm^2 for thiol concentrations of 0.1, 1 and 10mM, respectively, equating to an increase in binding of 321% from 0.1mM to 10mM concentrations.

FN adsorption decreased as a function of both increasing PEG-thiol MW and concentration (Figure 3b). FN binding was greatest for the 1k and 5k MW PEGs, both presenting similar FN binding to PPy-DS films modified at 0.1mM (2331 and 2379 ng/cm^2), 1mM (1874 and 1700 ng/cm^2) and 10mM (1849 and 1359 ng/cm^2) PEG-thiol concentrations, respectively (Figure 3b). PPy-DS modified with the 20k and 40k MW PEG-thiols demonstrated comparatively superior protein resistant properties, with the least FN binding demonstrated for the 10mM 40k MW treatment (118 ng/cm^2).

To further characterise the nature of the PEG adlayers organised on the PPy-DS surface, the mechanical properties of the PEG layers were examined by analysing the ratio between the two fundamental QCM-D measurement parameters, the frequency (f) and dissipation (D) (Figure 4). Analysis of the ΔD, which provides a measure of the dissipative properties of the adsorbed mass, with respect to the Δf (i.e., $\Delta D/\Delta f$ plot), provides information relating to the viscoelastic nature of the adsorbed layer, with a larger $\Delta D/\Delta f$ ratio indicative a more hydrated, viscoelastic adsorbed layer (Höök et al. 1998, Molino et al. 2012a). The $\Delta D/\Delta f$ ratio increased considerably as a function of increasing PEG-thiol MW, demonstrating the

adsorbed PEG layer to become increasingly hydrated and viscoelastic with increasing MW, resulting in a 'softer' surface bound molecular layer.

3.2.2 PEG-thiol Reaction Conditions

3.2.2.1 Temperature. We investigated the influence of temperature on both the overall mass of PEG-thiol binding to the PPy-DS surface, as well as the subsequent efficacy of the PEG modified PPy-DS film to resist FN adsorption. Figure 5 illustrates representative results for the modelled mass of PEG-thiol binding to the PPy-DS surface as a function of temperature (15, 25, 35 and 45°C) for each MW, as well as the subsequent FN adsorption to the modified polymers, as measured by QCM-D. The mass of PEG-thiol binding increased with increasing temperature for all PEG MWs. At 45ºC, PEG-thiol binding was 1037 ng/cm^2 for 1k, 1338 ng/cm^2 for 5k, 2007 ng/cm^2 for 20k and 2232 ng/cm^2 for 40k MWs, respectively.

FN adsorption followed a generally inverse relationship with the PEG-thiol binding, with FN adsorption decreasing as the PEG-thiol reaction temperature increased. For the 45°C PEG-thiol reaction treatments, FN adsorption was greatest for the 1k modified film (1942 ng/cm^2), followed by the 5k (1328 ng/cm^2) and 20k (1030 ng/cm^2) films, with the 40k MW film demonstrating the least FN adsorption (806 ng/cm^2), respectively. The efficacy of the temperature treatment as a method of enhancing the protein resistant properties of the PEG modified polymer was clear, with protein adsorption to the 45°C, compared to the 15°C, PEG-thiol treated films decreasing by ~17%, ~26%, ~36% and ~41% for 1k, 5k, 20k and 40k MW PEG-thiols, respectively.

3.2.2.2 Solvent. The influence of solvent on PEG-thiol binding to PPy-DS and gold was tested to determine the ability of engaging volatile solvents that may be more amenable to high throughput processes such as printing or dip coating (Figure 6). PEG-thiol binding to PPy-DS was slightly superior from aqueous, rather than ethanolic, media, with the same trend

evident for the gold substrate, however with a larger variation between treatments (Figure 6a).

Although FN adsorption to both the ethanolic and aqueous PEG-thiol treated gold surfaces was negligible, a significant difference was illustrated for the PPy-DS polymer. FN adsorption was greater on the PPy-DS polymer modified with PEG-thiol from the ethanolic solvent (~2650 ng/cm^2), compared to that from the aqueous solution (~1400 ng/cm^2) (Figure 6b).

3.2.2.3 Phosphine Catalysis. Phosphines have been reported to catalyze the addition of thiols to alkenes by an "assisted nucleophilic addition route" (Li et al. 2010). In order to see if such a mechanism was playing a role here, the water soluble phosphine TCEP was examined (Figure 7). Following 60 mins incubation with the PPy-DS film, TCEP alone (0.02 mM) demonstrated negligible binding to the polymer surface (~ 106 ng/cm^2), while PEG-thiol (0.1 mM 20k MW) with either 0.02 mM or 0.005 mM TCEP illustrated similar thiol binding to the control treatment (Figure 7a). However PPy-DS films modified with PEG-thiol in the presence of TCEP demonstrated a comparatively poor ability to resist protein binding compared to the control (Figure 7b), with protein adsorption increasing with an increase in TCEP concentration in the PEG-thiol aqueous solution during polymer modification. FN adsorption was greatest for the 0.02 mM TCEP control treatment (~ 2973ng/cm^2), followed by PEG-thiol modification with either 0.02mM (~ 2497ng/cm^2) or 0.005mM (1557 ng/cm^2) TCEP, respectively.

3.2.2.4 pH. The influence of solution pH on the degree of PEG-thiol binding to the PPy-DS surface was explored by buffering the aqueous solutions with di-sodium hydrogen orthophosphate to a pH of 8, 9 or 10. The QCM-D modelled mass data results from PEG-thiol binding (0.1mM 20k MW) to PPy-DS revealed pH to impart no significant influence on

the mass bound to the polymer surface, with measured values from all three pH treatments comparable to that of the DI water control (Figure 8). Although modelled mass values exhibited little change with pH, the $\Delta D/\Delta f$ ratio for PEG-thiol binding decreased incrementally with increasing pH, with the $\Delta D/\Delta f$ ratio for pH 8 (0.141 ± 0.001) and 9 (0.133 ± 0.009) both significantly greater than that for the PEG-thiol layer bound at pH 10 (0.117 ± 0.003) (Figure 8b). FN adsorption to the PEG-thiol modified films generally decreased as a function of pH during PEG-thiol modification, with the lowest FN adsorption illustrated for pH 9 (313 ± 69 ng/cm^2), followed by pH 10 (450 ± 79 ng/cm^2) and pH 8 (691 ± 167 ng/cm^2) PEG-thiol modification conditions, with the DI water control exhibiting the greatest FN binding (805 ± 110 ng/cm^2).

3.2.2.5 Fully Optimised PEG-thiol – PPy-DS Reaction Conditions: PEG-thiol binding, Protein Adsorption and Cellular interactions. In an attempt to enhance the efficiency of the PEG-thiol modification, we investigated the synergistic benefits of combining the optimised PEG-thiol reaction conditions determined herein for PEG-thiol MW, concentration, solvent, solution pH and reaction temperature. We undertook PEG-thiol modification experiments using the 40k MW PEG-thiol at a 1mM concentration in aqueous solution buffered to pH 9 at a temperature of 45 °C. While the 40k MW PEG-thiol did present enhanced PEG-thiol binding and protein resistance at a concentration of 10mM, we chose to employ the 1mM solution as the higher concentration presented a highly viscous solution that would prove difficult to employ for various fabrication techniques (i.e. inket and contact printing). PEG-thiol mass binding was 3604 ± 205 ng/cm^2, with a $\Delta D/\Delta f$ ratio of 0.1026 ± 0.0041. FN adsorption to the PEG-thiol modified polymer was 161 ± 98 ng/cm^2; significantly less than that presented on the unmodified control polymer (2572 ± 149 ng/cm^2) (Figure 9). We tested the efficacy of the PEG-thiol modification to resist a heterogeneous population of proteins using standard HAMS F10 cell culture media containing 20% fetal bovine serum. Protein

adsorption from the media to the PEG-thiol modified PPy-DS film (247 ± 84 ng/cm^2) was significantly less than that on the unmodified PPy-DS surface (2093 ± 314), illustrating an 88% decrease in protein adsorption to the polymer surface (Figure 9). The optimised PEG-thiol modification conditions were further investigated for their ability to prevent cell adhesion and proliferation on the polymer surface. Figure 10 presents images of primary mouse skeletal myoblasts seeded at a concentration of 30,000 cells/cm^2 onto PPy-DS films for which only half the film was modified with PEG-thiol using the above optimised conditions. After 3 days, cell adhesion and proliferation was almost completely inhibited on the PEG-thiol modified regions of the polymer (Figure 10).

4. Discussion

4.1 *Efficacy of PEG for Protein Resistance*

It is widely accepted that the ability of PEG to resist protein interactions is attributed to a combination of steric repulsion (i.e. conformational flexibility and mobility) and high hydration, or water structuring, which presents an *inert* substrate to the surrounding environment and produces a steric exclusion zone at the substratum (Harder et al. 1998, Heuberger et al. 2004, Pasche et al. 2003). The interplay between PEG grafting density on the surface and the intermolecular interactions of tethered PEG molecules has been shown to be particularly critical in optimizing surface coverage and molecular conformation that drives the protein resistant properties of the PEG adlayer (Kingshott et al. 2002, Sofia et al. 1998, Szleifer 1997). PEG adsorbed at low densities on a substratum is proposed to present a mushroom-like regime on the surface, unconstrained by interactions with neighbouring molecules. In this condition, the PEG molecule and the coupled solvation shell do not contact each other and fail to completely cover the underlying substratum, allowing proteins of suitable size to manoeuvre between PEG chains and reach the underlying surface, drawn by

attractive forces such as van der Waals, electrostatic and hydrophobic interactions. Increasing the PEG density at the surface decreases the free space between PEG chains, forcing neighbouring chains, along with their solvation shell, to overlap. In this state, intermolecular repulsive interactions force the elongation of the surface tethered PEG molecule away from the substratum. This results in a regime shift of the PEG molecule from a mushroom- to a brush type conformation (Prime & Whitesides 1993). The overlapping of the surface tethered PEG chains is believed to provide an enhanced surface coverage that prevents protein from reaching the underlying substratum

4.2 Modification of PPy with PEG-thiol

We employed PEG-thiols of varying MW to investigate the influence of PEG chain length on the ability of PEG to inhibit protein adsorption to PPy-DS. The efficacy of PEG to resist FN adsorption to PPy was clearly differentiated by MW, with FN resistance increasing with increasing PEG MW (Figure 3). PEG MW, or chain length, has previously been shown to influence the ability of PEG to resist protein interactions, with larger MW PEG demonstrated to be more effective at inhibiting protein adsorption to the underlying substratum (Prime & Whitesides 1993). An increased PEG chain length is proposed to improve steric repulsion by increasing the overall exclusion distance between the protein and the underlying substratum, as well as enhancing overall surface coverage and molecular organisation within the surface bound PEG layer.

In addition, increasing the MW of PEG considerably increased the $\Delta D/\Delta f$ ratio of the PEG layer (Figure 4). As noted previously, the $\Delta D/\Delta f$ ratio provides information regarding the viscoelastic properties, or hydration, of the surface-bound layer (Höök et al. 1998). The increase in the $\Delta D/\Delta f$ ratio with increasing PEG-thiol MW denotes an expected increase in hydration, and thus viscoelasticity, of the surface-bound molecules as their chain length

increases. This may additionally act to enhance PEG mobility and osmotic repulsion as the PEG chains become longer and more hydrated, dissuading protein binding at the polymer interface.

Several studies (Harder et al. 1998, Herrwerth et al. 2003, Kingshott et al. 2002, Ngadi et al. 2008, Pasche, De Paul et al. 2003, Sofia et al. 1998) however, have identified both PEG MW, and surface density, as critical to determining the ability of PEG layers to inhibit interfacial protein adsorption. The relatively minor difference in overall PEG-thiol binding mass, relative to the difference in PEG MW (e.g. 1506ng/cm^2 and 6197ng/cm^2 for 1k and 40k PEG at 10mM, respectively), is much lower than what would be expected for surface binding at equivalent densities. We therefore suggest that the surface density of PEG-thiol on the PPy surface to be significantly greater for the smaller MW PEGs. However, even at the proposed highest PEG-thiol binding densities, the 1k MW PEG fails to act as an effective inhibiter of interfacial protein adsorption compared to the large MW PEGs studied here.

It is critical to note that the binding density of PEG-thiol to the ICP surface is limited by the density of possible reactive sites along the PPy backbone. Therefore, unlike standard model systems that have traditionally been employed to study surface tethered PEG layers, including block co-polymers and self-assembled monolayers on metallic substrates, the surface density of PEG on inherently conducting polymers is not only governed by intra- and intermolecular interactions of the adsorbent during the surface binding process, but also on the availability and spatial distribution of *binding* or *reaction* sites on the polymer surface. The distribution of these sites can be influenced by several factors, including polymer oxidation state and the counterion concentration at the polymer surface. While the spacing between binding sites on the PPy backbone are theoretically estimated to be ~200 pm, the presence of the polymeric counterion at the composite surface can occupy as much as several square nm's (Gelmi et al. 2012). Therefore, the polymer interface presents a montage of

reactive (PPy) regions for PEG-thiol binding, dispersed amongst non-reactive (DS) regions. This is in marked contrast to inorganic surfaces, such as gold, where the density of reactive sites is far higher, resulting in close packing of even short molecular chains.

To effectively modify the PPy-DS surface, the PEG coating must efficiently protect both the PPy and biopolymer regions of the polymer exposed at the material interface. One method of achieving this is to reach PEG densities at the substrate that produce an overlapping of PEG chains and their respective solvation shells, producing a more confluent coverage of PEG on the surface. Increasing the surface density of surface tethered PEG has been proposed to result in the overlapping of PEG chains, causing the elongation and dehydration of PEG on the surface as intermolecular repulsion between surface tethered chains acts to drive PEG conformation from a mushroom- to a brush-like regime (Prime & Whitesides 1993). Figure 4 illustrates the $\Delta D/\Delta f$ ratio of the PEG-thiol layer as a function of PEG MW and thiol concentration during deposition. Both the 1k and 5k MW PEG demonstrate a clear reduction in the $\Delta D/\Delta f$ ratio as the concentration of the PEG in solution increases (i.e. as PEG mass on the surface increases), indicating that the increase in surface density (PEG binding) as thiol concentration in the aqueous solution increases generates sufficient PEG binding densities at which significant intermolecular interactions are achieved. This effect however, is largely absent for the 20k and 40k MW treatments, where an increase in PEG-thiol binding was not accompanied by a significant reduction in $\Delta D/\Delta f$ ratio (Figure 4).

Although the smaller MW PEG-thiol treatments achieved surface densities sufficient to induce PEG-PEG interactions and rigidification of the adlayer, only a modest reduction in FN binding was illustrated. We propose the failure of the 1k and 5k MW PEG-thiol treatments to effectively inhibit FN interactions with the surface lies in their inability to provide an adequate separation distance or steric exclusion zone between the protein and PPy-DS surface, allowing protein – polymer attractive forces to overcome the steric obstacles and

bind to the PPy surface. Additionally, because PEG-thiol reaction sites on the polymer surface are interspersed with non-reactive *island* or *zones* likely to be several square nm's in area (dopant rich areas), their respective chain lengths may be inadequate to shield or cover these regions on the polymer surface. Although the 20k and 40k PEG-thiol treatments did not appear to reach a density at which intermolecular interactions may act to enhance surface coverage of the adlayer, the likely increase in the 2- and 3-dimensional exclusion zone around each *binding* site may provide a mechanism by which neighbouring non-reactive sites may be afforded protection as the PEG molecules fan out across the substratum from the binding site. We therefore propose that both a high MW PEG and high surface binding density are the critical parameters required for the development of a protein resistant PEG adlayer on PPy.

4.3 Improving the Efficacy of PEG – PPy Modification

We employed several methods in an attempt to increase the efficiency of PEG-thiol binding to the PPy-DS interface, including varying the reaction conditions (temperature and solvent) and employing several catalytic compounds and treatments. Increasing the reaction temperature between 15 - 45ºC resulted in an incremental increase in PEG-thiol binding, and decrease in FN adsorption, for all PEG compounds (Figure 5). Employing the 20k MW PEG-thiol as a standard, increasing the temperature from 15 - 45 ºC improved PEG binding by ~29% and decreased FN adsorption by ~39%, demonstrating temperature to be an effective method of improving PEG-thiol binding to PPy-DS. The higher temperature may increase the extent of the thiol coupling reaction by increasing the mobility of the free thiols in solution as well and increasing the overall yield of the reaction. Increasing the PEG-thiol solution temperature is also known to decrease PEG solubility and interchain repulsion, allowing a tighter packing of PEG molecules at the substratum surface (Dalsin et al. 2005, Prime & Whitesides 1993), and we suggest this mechanism may be operative here.

Both ethanolic and aqueous solutions of PEG-thiol were used to determine whether there was any change in thiol binding as a function of solvent. Figure 6 reveals that PEG-thiol binding from the aqueous solvent provided greater binding on both PPy-DS and piranha cleaned gold (employed as a control). Although surface modification from both solvent treatments were effective at eliminating FN adsorption to the gold substrate (Figure 6), the PEG modification from the ethanolic solution on PPy-DS performed poorly, exhibiting an increase in FN binding of ~ 89% compared to surface PEG modification from an aqueous solution.

To improve the efficiency of the thiol – PPy reaction, we probed the underlying mechanism/s governing this reaction by employing a range of catalytic treatments and compounds to promote PEG-thiol binding with the polymer surface. The secondary and tertiary amines, as well as the phosphine TCEP has been used to enhance the rate of Michael additions between thiols and electron-deficient alkenes. Here however, TCEP had a negligible effect on mass binding to PPy-DS (Figure 7). Interestingly, the presence of the compound had a substantial inhibitory effect on the ability of the composite surface to resist protein adsorption to the PPy-DS surface. The reason for this is not clear, though the reagent may have served to decrease the pH at the surface and thus, affecting the packing of the PEG chains.

Increasing the pH of the aqueous PEG-thiol solution significantly influenced both the viscoelasticity and protein resistance of the PEG layer (Figure 8). While no significant increase in the total adsorbed mass compared to the control was evident, the $\Delta D/\Delta f$ ratio decreased with increasing pH. It is important to note that QCM-D measures the hydrated mass of the adsorbed species and therefore the modelled mass represents both the PEG-thiol and the water hydrodynamically coupled to the surface bound layer. As the pH increases, there is a concomitant decrease in the $\Delta D/\Delta f$ ratio. It has been demonstrated that a decrease in the $\Delta D/\Delta f$ ratio is indicative of a decrease in hydration of the adsorbed layer, and therefore while the overall *measured* mass for all pH treatments are comparable, we suggest that the

percentage of the mass attributable to the PEG increases as the pH increases, representing an increase in PEG density on the polymer surface. Unfortunately, this assertion is difficult to test, as altering the pH after the thiol deposition not only affects the organization of the thiol, but also impacts the underlying film. The relative contributions to the QCM data cannot be quantified.

4.3 *Optimisation of PPy PEG-thiol Modification: Efficacy at Inhibiting Protein and Cellular Adhesion*

We combined the optimised PEG-thiol reaction conditions identified for each of the tested parameters to determine whether we could further enhance the PEG-thiol modification of the PPy-DS polymer (Figure 9). The 40k MW PEG-thiol was employed as it demonstrated the greatest protein resistant properties of all PEG MWs tested. Under the optimised PEG-thiol reaction conditions (1mM aqueous solution at pH 9 and 45°C) the mass of PEG-thiol binding to the PPy-DS surface (3604 ± 205 ng/cm^2) was considerably higher than that demonstrated for the same PEG MW and concentration deposited under ambient conditions (25°C) (~2720 ng/cm^2), however less than adsorbed at a 10mM concentration (~6197 ng/cm^2). The efficacy of the optimised PEG-thiol modification to resist FN adsorption (161 ± 98 ng/cm^2) is comparable to that demonstrated by the 10mM 40k PEG-thiol modification in aqueous solution at 25°C (~118 ng/cm^2). Additionally, the optimised PEG modification was effective at resisting the adsorption of proteins from cell culture media containing 20% FBS serum, demonstrating a decrease of 88% compared to the unmodified control PPy-DS film (Figure 9). The reduction in the $\Delta D/\Delta f$ ratio for 40k MW PEG-thiol deposited under optimised conditions (0.1026 ± 0.0041) is considerably less than that presented for 40k MW PEG-thiol at both 1mM and 10mM concentrations ($\Delta D/\Delta f$ of ~0.16). As discussed previously, a reduction in the $\Delta D/\Delta f$ is indicative of a decrease in adlayer hydration and therefore an increase in the percentage mass of PEG in the adlayer. As such, we propose the proportion of

mass attributed to the PEG-thiol bound under the fully optimised conditions is greater than that demonstrated even for the 10mM 40k MW treatment in aqueous solution.

The significant reduction in protein adsorption resulting from the optimised PEG-thiol modification is clearly adequate to prevent cellular adhesion during initial seeding, and subsequent migration to the modified regions of the polymer, with unmodified areas demonstrating a dense coverage of cells after 3 days, with a clear boundary evident where the primary skeletal muscle cells have been unable to adhere and proliferate (Figure 10).

5. Mechanistic Observations

We have previously reported that thiols rapidly react with various ICPs and, in the case of polypyrrole, the reaction is an irreversible addition (Molino et al. 2012). A permanent reduction in the conductivity of the polymer is observed, strongly suggesting that the thiol adds to the backbone to give a covalent C-S linkage that disrupts the conjugation of the π-system. The reaction is largely independent of the polymer dopant and should probably be viewed as a hydrothiolation of an alkene. This “thiol-ene” reaction is thought to occur by at least three distinct mechanisms, depending on the reactants and conditions (Hoyle & Bowman 2010, Lowe 2010). Most commonly, this is a radical reaction and is frequently photoinitiated (Hoyle et al. 2004, Niels ten et al. 2008). This approach is particularly useful with electron-rich alkenes and situations where the radicals do not produce undesired side reactions. There are also many examples of base-catalyzed thiol-ene reactions, particularly with electron-poor alkenes (Mather et al. 2006). In cases where the base-catalyzed process is unsatisfactory, nucleophilic-initiated versions of the reaction have been developed, where the reaction rate is enhanced under mild conditions by the additions of amines or phosphines (Chan et al. 2010, Hoyle & Bowman 2010, Lowe 2010).

The conducting form of polypyrroles and polythiophenes consist of an oxidized conjugated backbone that contains both delocalized cations and radicals. It is easy to envision either a radical or ionic mechanism playing the dominant role in the thiol addition process and there is precedence for the polymer reacting with both types of reagents. For example, the reduced form of PPy has been used as an anti-oxidant (Hsu et al. 2011), while the conducting form oxidizes the reducing thiols dithiothreitol and glutathione to disulfides (Thomas et al. 2000). Radical additions of thiols to alkenes are favored with electron-rich systems, but this is decidedly not the case with cationic conducting polymers, decreasing the likelihood of a radical process. We attempted to examine the effect of UV irradiation at various wavelengths on the rate of thiol addition (data not shown) using the QCM. However, both polypyrrole and PEDOT films showed significant drift in both the frequency and resonance dampening, preventing meaningful analysis. This is consistent with previous reports showing that long wavelength light encourages the degradation of the film in aqueous solutions.

An ionic mechanism is more consistent with our observations and with literature reports on the thiol addition to electron-poor systems. The QCM results suggest that increase pH does increase the overall extent of deposition, though the interpretation of these data is complicated by changes in the hydration of the PEG moieties. Increased pH will increase the nucleophilicity of the thiol, though too great of an increase will result in degradation due to competitive hydroxide ion attack on the polypyrrole (Forsyth & Truong 1995). Attempts to further improve the reaction using a phosphine-catalyzed reaction proved counter productive, either due to a decrease in pH or perhaps a side reaction due to phosphine attack on the polymer (Zhang & Kohn 2012).

6. Conclusions

Optimization of the PEG-thiol reaction conditions with PPy-DS leads to a highly effective procedure for reducing both protein adsorption and cell attachment to the conducting polymer composite surface. These optimization conditions are also amenable to patterning and the use of mixed thiols to form chemical gradients on the polymer surface. Conducting polymers are versatile materials through which material physicochemical and electrochemical properties may be tuned in order to tailor materials for a range of applications. They are known to exhibit inherent anti-corrosive properties, and can draw on a suite of existing fabrication techniques to create stand-alone materials, or for their incorporation into existing coatings technologies. PEG functionalised conducting polymer materials are an exciting class of materials that show promise not only in the field of biomedical materials, but as a flexible fouling resistant material platform to be employed for an array of aquatic applications.

Acknowledgements

The authors gratefully acknowledge the Australian Research Council and the National Health and Medical Research Council (Grant No. 573430). PJM acknowledges funding support through the Vice Chancellors Fellowship award (UOW). TWH thanks the Australian–American Fulbright Commission for a scholarship supporting this work. We also acknowledge the Australian National Nanofabrication Facility (ANFF) for access to equipment.

References

Abidian MR, Martin DC. 2009. Multifunctional Nanobiomaterials for Neural Interfaces. Advanced Functional Materials. 19(4):573-585.

Aizawa Y, Owen SC, Shoichet MS. 2012. Polymers used to influence cell fate in 3D geometry: New trends. Progress in Polymer Science. 37(5):645-658.

Alves NM, Pashkuleva I, Reis RL, Mano JF. 2010. Controlling cell behavior through the design of polymer surfaces. Small. 6(20):2208-2220.

Bergman B, Hanks TW. 2000. Spectroscopic, Microscopic, and Surface Analysis of Alkanethiol- and Fluoroalkanethiol-Modified Conducting Polymer Thin Films. Macromolecules. 33(21):8035-8042.

Bixler GD, Bhushan B. 2012. Biofouling: lessons from nature. Philos Trans A Math Phys Eng Sci. 370(1967):2381-2417.

Chan JW, Hoyle CE, Lowe AB, Bowman M. 2010. Nucleophile-Initiated Thiol-Michael Reactions: Effect of Organocatalyst, Thiol, and Ene. Macromolecules. 43(15):6381-6388.

Dalsin JL, Lin L, Tosatti S, Voros J, Textor M, Messersmith PB. 2005. Protein resistance of titanium oxide surfaces modified by biologically inspired mPEG-DOPA. Langmuir. 21(2):640-646.

Falconnet D, Csucs G, Grandin HM, Textor M. 2006. Surface engineering approaches to micropattern surfaces for cell-based assays. Biomaterials. 27(16):3044-3063.

Forsyth M, Truong VT. 1995. A study of acid/base treatments of polypyrrole films using 13C n.m.r. spectroscopy. Polymer. 36(4):725-730.

Geckil H, Xu F, Zhang X, Moon S, Demirci U. 2010. Engineering hydrogels as extracellular matrix mimics. Nanomedicine (Lond). 5(3):469-484.

Gelmi A, Higgins MJ, Wallace GG. 2010. Physical surface and electromechanical properties of doped polypyrrole biomaterials. Biomaterials. 31(8):1974-1983.

Gelmi A, Higgins MJ, Wallace GG. 2012. Attractive and repulsive interactions originating from lateral nanometer variations in surface charge/energy of hyaluronic acid and chondroitin sulfate doped polypyrrole observed using atomic force microscopy. J Phys Chem B. 116(45):13498-13505.

Glinel K, Thebault P, Humblot V, Pradier CM, Jouenne T. 2012. Antibacterial surfaces developed from bio-inspired approaches. Acta Biomater. 8(5):1670-1684.

Green RA, Lovell NH, Wallace GG, Poole-Warren LA. 2008. Conducting polymers for neural interfaces: challenges in developing an effective long-term implant. Biomaterials. 29(24-25):3393-3399.

Hanks T, Glish L, Singh S, Johnson D, Wright L. 2005. Conducting polymers as substrates for surface-mounted molecular devices. Synthetic Metals. 153(1–3):177-180.

Harder P, Grunze M, Dahint R, Whitesides GM, Laibinis PE. 1998. Molecular Conformation in Oligo(ethylene glycol)-Terminated Self-Assembled Monolayers on Gold and Silver Surfaces Determines Their Ability To Resist Protein Adsorption. The Journal of Physical Chemistry B. 102(2):426-436.

Herrwerth S, Eck W, Reinhardt S, Grunze M. 2003. Factors that Determine the Protein Resistance of Oligoether Self-Assembled Monolayers − Internal Hydrophilicity, Terminal Hydrophilicity, and Lateral Packing Density. Journal of the American Chemical Society. 125(31):9359-9366.

Heuberger M, Drobek T, Vörös J. 2004. About the Role of Water in Surface-Grafted Poly(ethylene glycol) Layers. Langmuir. 20(22):9445-9448.

Higgins MJ, Molino PJ, Yue Z, Wallace GG. 2012. Organic Conducting Polymer–Protein Interactions. Chemistry of Materials. 24(5):828-839.

Höök F, Rodahl M, Brzezinski P, Kasemo B. 1998. Energy Dissipation Kinetics for Protein and Antibody−Antigen Adsorption under Shear Oscillation on a Quartz Crystal Microbalance. Langmuir. 14(4):729-734.

Hoyle CE, Bowman CN. 2010. Thiol–Ene Click Chemistry. Angewandte Chemie International Edition. 49(9):1540-1573.

Hoyle CE, Lee TY, Roper T. 2004. Thiol–enes: Chemistry of the past with promise for the future. Journal of Polymer Science Part A: Polymer Chemistry. 42(21):5301-5338.

Hsu CF, Peng H, Basle C, Travas-Sejdic J, Kilmartin PA. 2011. ABTS•+ scavenging activity of polypyrrole, polyaniline and poly(3,4-ethylenedioxythiophene). Polymer International. 60(1):69-77.

Khan S, Newaz G. 2010. A comprehensive review of surface modification for neural cell adhesion and patterning. J Biomed Mater Res A. 93(3):1209-1224.

Kingshott P, Thissen H, Griesser HJ. 2002. Effects of cloud-point grafting, chain length, and density of PEG layers on competitive adsorption of ocular proteins. Biomaterials. 23(9):2043-2056.

Li G-Z, Randev RK, Soeriyadi AH, Rees G, Boyer C, Tong Z, Davis TP, Becer CR, Haddleton DM. 2010. Investigation into thiol-(meth)acrylate Michael addition reactions using amine and phosphine catalysts. Polymer Chemistry. 1(8):1196-1204.

Lowe AB. 2010. Thiol-ene "click" reactions and recent applications in polymer and materials synthesis. Polymer Chemistry. 1(1):17-36.

Lühmann T, Hall H. 2009. Cell Guidance by 3D-Gradients in Hydrogel Matrices: Importance for Biomedical Applications. Materials. 2(3):1058-1083.

Ma Z, Mao Z, Gao C. 2007. Surface modification and property analysis of biomedical polymers used for tissue engineering. Colloids Surf B Biointerfaces. 60(2):137-157.

Mather BD, Viswanathan K, Miller KM, Long TE. 2006. Michael addition reactions in macromolecular design for emerging technologies. Progress in Polymer Science. 31(5):487-531.

Meyers SR, Grinstaff MW. 2012. Biocompatible and bioactive surface modifications for prolonged in vivo efficacy. Chem Rev. 112(3):1615-1632.

Molino PJ, Higgins MJ, Innis PC, Kapsa RM, Wallace GG. 2012a. Fibronectin and bovine serum albumin adsorption and conformational dynamics on inherently conducting polymers: a QCM-D study. Langmuir. 28(22):8433-8445.

Molino PJ, Wallace GG, Hanks TW. 2012b. Hydrophobic conducting polymer films from post deposition thiol exposure. Synthetic Metals. 162(15–16):1464-1470.

Ngadi N, Abrahamson J, Fee C, Morison K. 2008. QCM-D study on the relationship of PEG coated stainless steel surfaces to protein resistance. Interanational Journal of Chemical and Biological Engineering. 1(3):125-129.

Niels ten B, Christina D, Helmut S. 2008. Thiol−Ene Modification of 1,2-Polybutadiene Using UV Light or Sunlight. Macromolecules. 41(24):9946-9947.

Palacio ML, Bhushan B. 2012. Bioadhesion: a review of concepts and applications. Philos Trans A Math Phys Eng Sci. 370(1967):2321-2347.

Pasche S, De Paul SM, Vörös J, Spencer ND, Textor M. 2003. Poly(l-lysine)-graft-poly(ethylene glycol) Assembled Monolayers on Niobium Oxide Surfaces: A Quantitative Study of the Influence of Polymer Interfacial Architecture on Resistance to Protein Adsorption by ToF-SIMS and in Situ OWLS. Langmuir. 19(22):9216-9225.

Patil JS, Kamalapur MV, Marapur SC, Kadam DV. 2010. Ionotropic gelation and polyelectrolyte complexation: the novel techniques to design hydrogel particulate sustained, modulated drug delivery system: a review. Digest Journal of Nanomaterials and Biostructures. 5(1):8.

Prime KL, Whitesides GM. 1993. Adsorption of proteins onto surfaces containing end-attached oligo(ethylene oxide): a model system using self-assembled monolayers. Journal of the American Chemical Society. 115(23):10714-10721.

Ravichandran R, Sundarrajan S, Venugopal JR, Mukherjee S, Ramakrishna S. 2010. Applications of conducting polymers and their issues in biomedical engineering. J R Soc Interface. 7 Suppl 5:S559-579.

Roach P, Parker T, Gadegaard N, Alexander MR. 2010. Surface strategies for control of neuronal cell adhesion: A review. Surface Science Reports. 65(6):145-173.

Sofia SJ, Premnath V, Merrill EW. 1998. Poly(ethylene oxide) Grafted to Silicon Surfaces: Grafting Density and Protein Adsorption. Macromolecules. 31(15):5059-5070.

Svirskis D, Travas-Sejdic J, Rodgers A, Garg S. 2010. Electrochemically controlled drug delivery based on intrinsically conducting polymers. J Control Release. 146(1):6-15.

Szleifer I. 1997. Polymers and proteins: interactions at interfaces. Current Opinion in Solid State and Materials Science. 2(3):337-344.

Thomas CA, Zong K, Schottland P, Reynolds JR. 2000. Poly(3,4-alkylenedioxypyrrole)s as Highly Stable Aqueous-Compatible Conducting Polymers with Biomedical Implications. Advanced Materials. 12(3):222-225.

Vladkova TG. 2010. Surface Engineered Polymeric Biomaterials with Improved Biocontact Properties. International Journal of Polymer Science. 2010.

Yu LMY, Leipzig ND, Shoichet MS. 2008. Promoting neuron adhesion and growth. Materials Today. 11(5):36-43.

Zhang N, Kohn DH. 2012. Using polymeric materials to control stem cell behavior for tissue regeneration. Birth Defects Res C Embryo Today. 96(1):63-81.

Figures

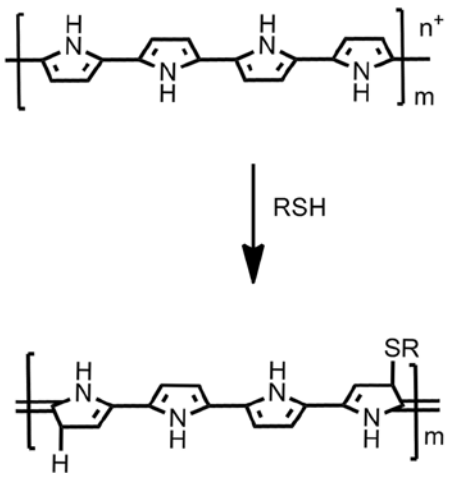

Figure 1.

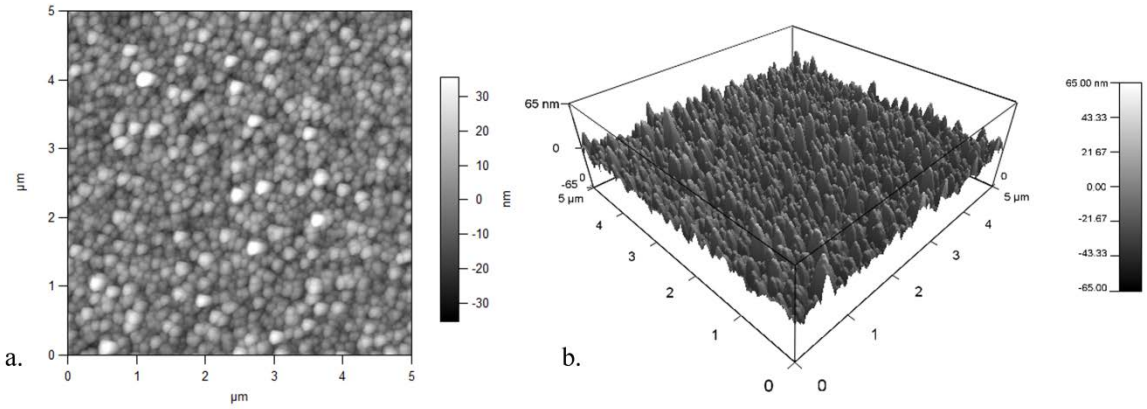

Figure 2.

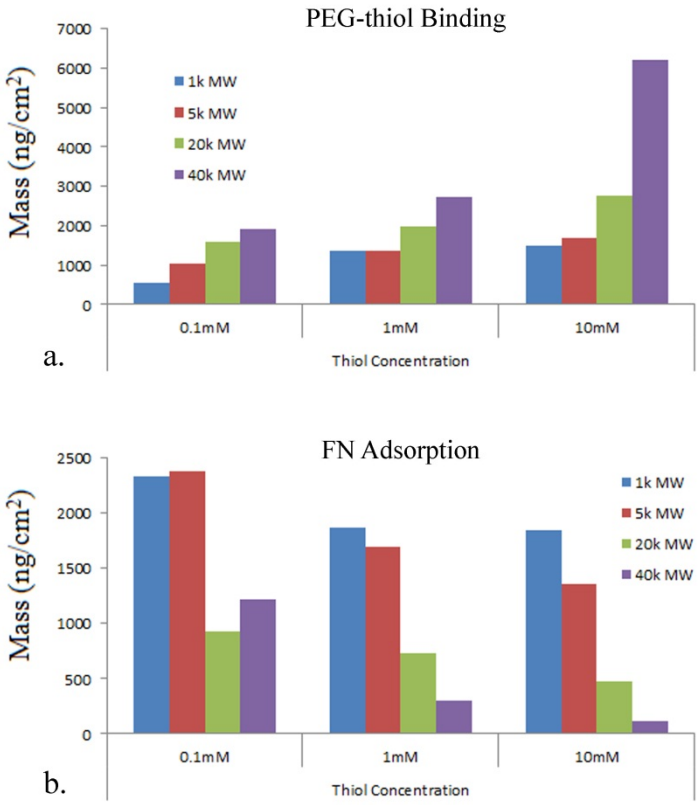

Figure 3.

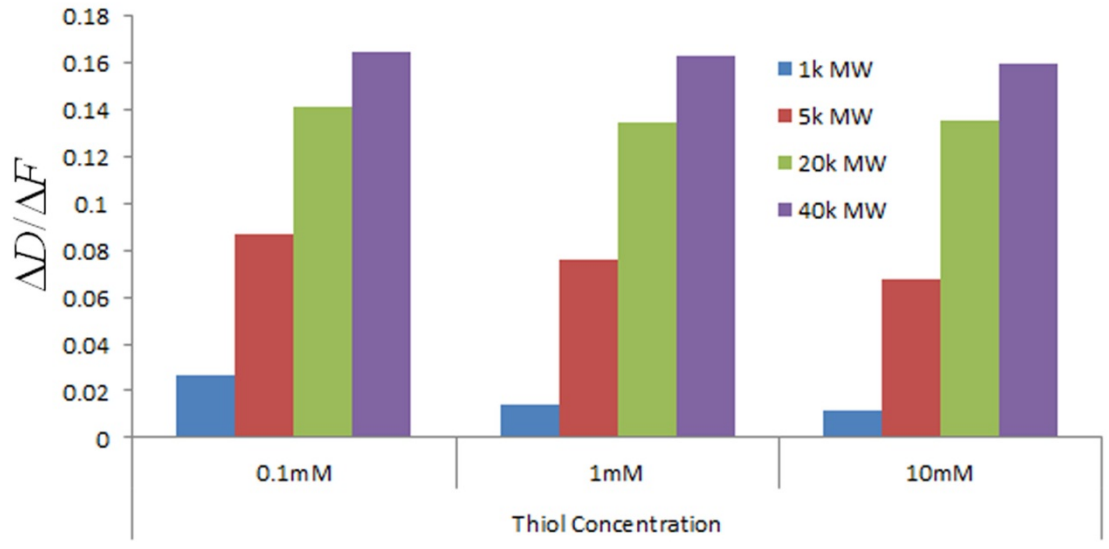

Figure 4.

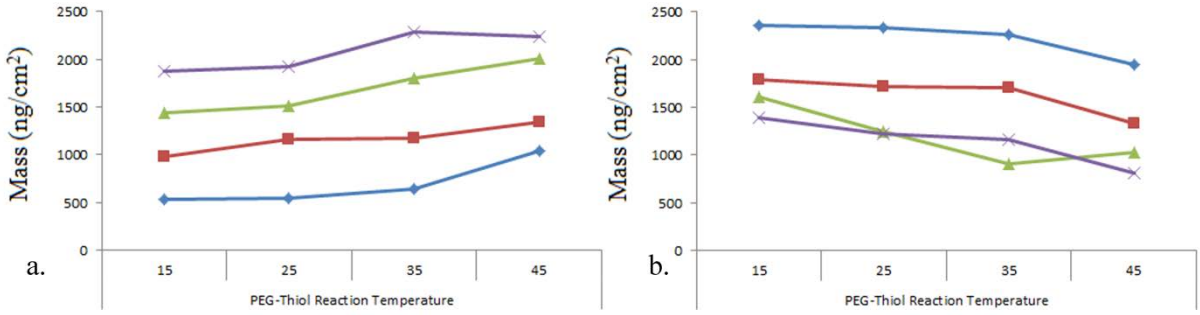

Figure 5.

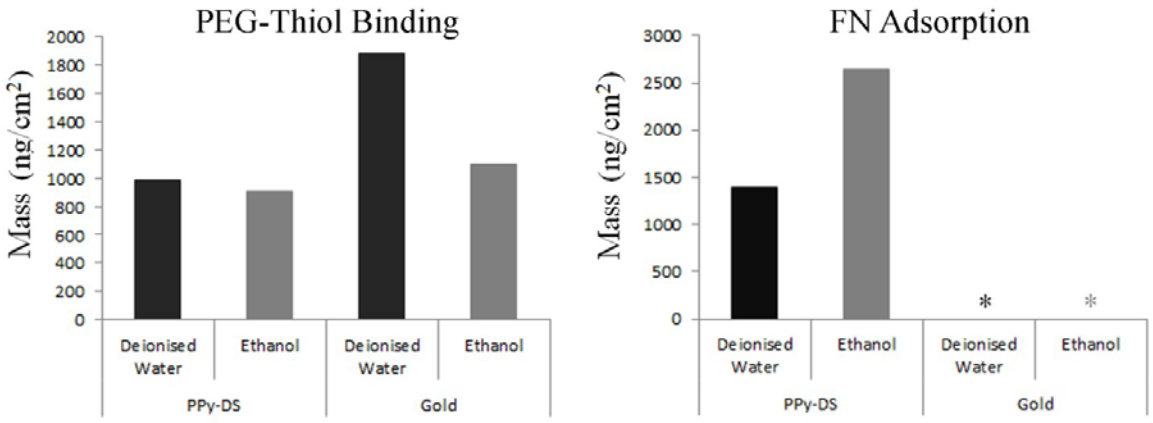

Figure 6.

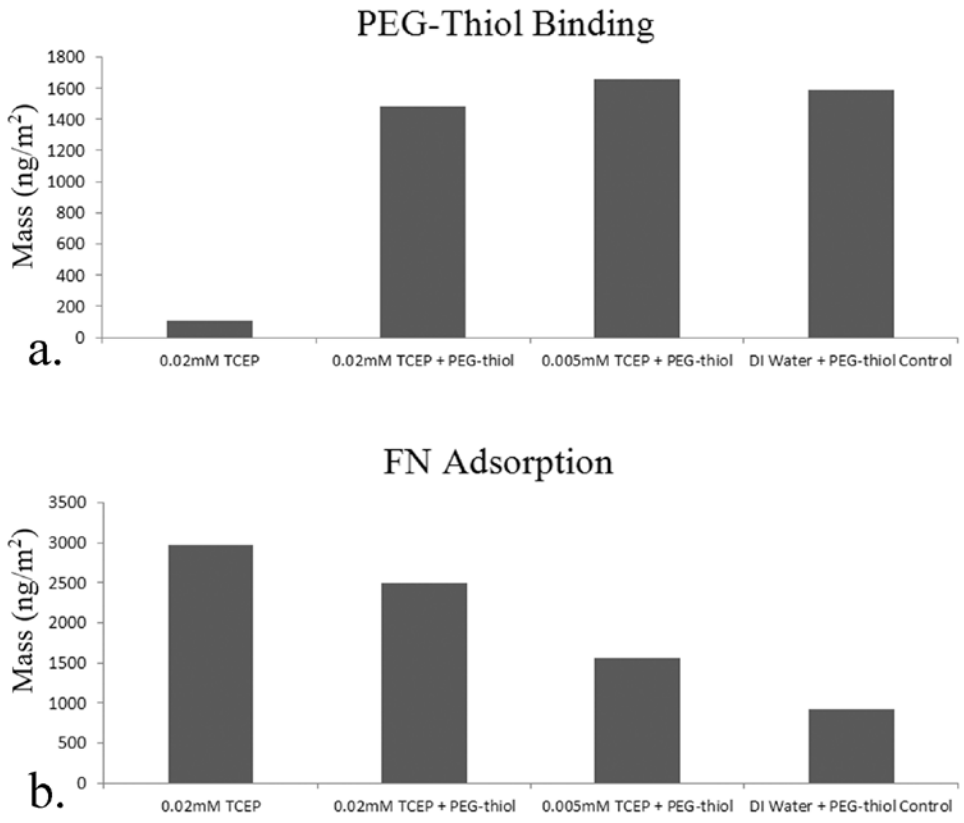
PEG-Thiol Binding
Mass (ng/m²)
1800
1600
1400
1200
1000
800
600
400
200
0
a.
0.02mM TCEP
0.02mM TCEP + PEG-thiol
0.005mM TCEP + PEG-thiol
DI Water + PEG-thiol Control
FN Adsorption
Mass (ng/m²)
3500
3000
2500
2000
1500
1000
500
0
b.
0.02mM TCEP
0.02mM TCEP + PEG-thiol
0.005mM TCEP + PEG-thiol
DI Water + PEG-thiol Control

Figure 7.

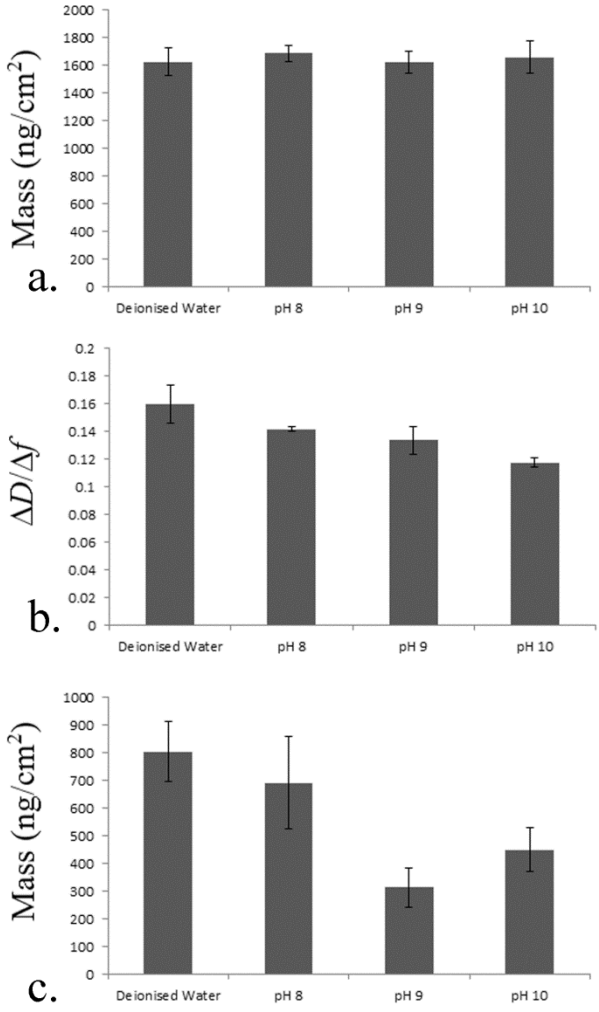

Figure 8.

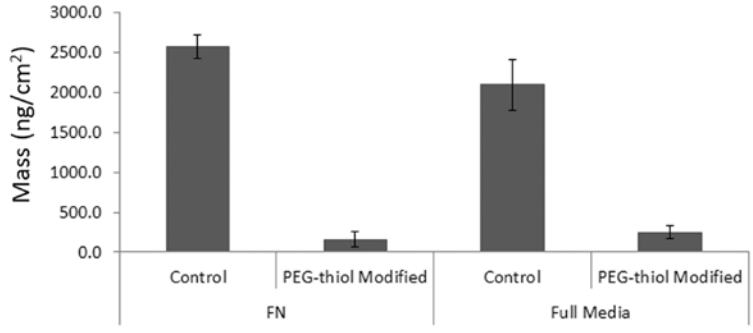

Figure 9.

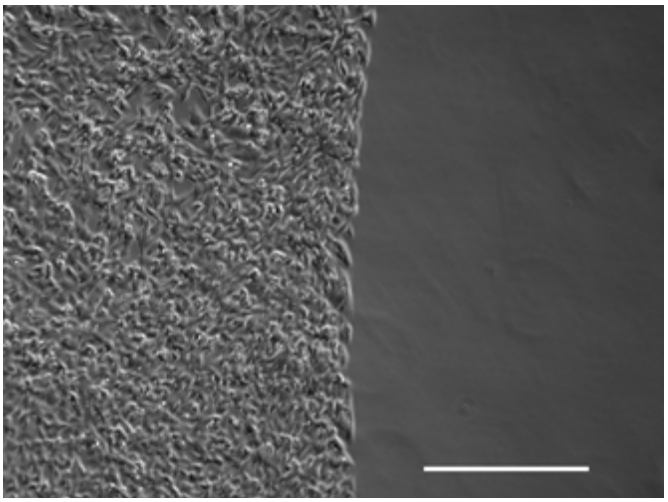

Figure 10.

Figure Captions

Figure 1. Proposed mechanism for the PEG-thiol/polypyrrole reaction.

Figure 2. AFM images of PPy-DS polymer films, with data presented in both 2D (a) and 3D (b) to illustrate surface morphology and interfacial topography. Scans are 5µm X 5µm.

Figure 3. a. PEG-Thiol Modification to PPy-DS polymer films as a function of MW and PEG-thiol concentration. **b.** FN Adsorption to PPy-DS films modified PEG-thiol as a function of MW and concentration. Both PEG-thiol and FN binding to the PPy-DS surface is presented as ng/cm^2 as measured using QCM-D.

Figure 4. $\Delta D/\Delta f$ of PEG-thiol modification of PPy-DS films at 0.1mM, 1mM and 10mM for 1k, 5k, 20k and 40k MW PEG.

Figure 5. PEG-Thiol Modification of PPy-DS (a) and subsequent FN binding to modified polymer (b) as a function of reaction temperature and mPEG molecular weight (1k (♦), 5k (■), 20k (▲) and 40k (×)). Both PEG-thiol and FN binding to the PPy-DS surface presented as ng/cm^2 as measured using QCM-D.

Figure 6. a. PEG-thiol binding (0.1mM 20k MW) to PPy-DS and gold in either aqueous or ethanolic solutions. b. FN adsorption to PPy-DS and gold PEG-thiol modified surfaces.

Figure 7. a. PEG-thiol binding (0.1mM 20k MW) to PPy-DS as a function of TCEP concentration. **b.** FN adsorption to PEG (TCEP) treated PPy-DS films.

Figure 8. a. Mass of PEG-thiol binding (0.1mM 20k MW) to PPy-DS as a function of solution pH. **b.** $\Delta D/\Delta f$ ratio for surface bound PEG-thiol layer on PPy-DS for each treatment. **c.** FN adsorption to the PEG modified PPy-DS films. Error bars represent 95% confidence intervals around the mean.

Figure 9. Mass of protein adsorption to PPy-DS polymer films with/without modification with PEG. PEG-thiol modification undertaken with 40k MW PEG at 1mM concentration at pH 9 and 45°C. Protein adsorption studied using FN (50ug/ml in PBS) or Full Media (HAMS F10 with 20 % FBS). Error bars represent 95% confidence intervals around the mean.

Figure 10. Colonisation of PEG—thiol modified PPy-DS by primary mouse skeletal muscle cells. (unmodified (left) and modified (right) polymer regions.) Scale bar represents 400µm.